



# Hydrogen absorption and desorption in the Mg–Ag system



Guillermina Urretavizcaya\*, Ana C. Sarmiento Chávez, Facundo J. Castro

Centro Atómico Bariloche (CNEA, CONICET), Instituto Balseiro (UNCuyo, CNEA), Av. Bustillo 9500, R8402AGP, S.C. de Bariloche, Río Negro, Argentina

## ARTICLE INFO

### Article history:

Received 25 November 2013

Received in revised form 7 May 2014

Accepted 9 May 2014

Available online 22 May 2014

### Keywords:

Hydrogen absorbing materials

Intermetallics

Mechanical milling

Thermodynamic destabilization

Reaction pathway

Kinetics

## ABSTRACT

We analyze hydrogen absorption and desorption in Mg and Mg–Ag compounds prepared by mechanical milling. The materials were obtained by processing mixtures of Mg or MgH<sub>2</sub> with different proportions of Ag under Ar or H<sub>2</sub> atmosphere. We observe that Ag and AgMg destabilize MgH<sub>2</sub>. In the first case the products of the reaction of Ag and MgH<sub>2</sub> are AgMg and H<sub>2</sub>, in the second case MgH<sub>2</sub> reacts with AgMg to give AgMg<sub>4</sub> and H<sub>2</sub>. The first reaction was only observed in the forward direction, whereas the second one was registered in both directions. The impossibility to reverse the first reaction was attributed to poor kinetics and experimental limitations. The reversible destabilization induced by AgMg is low, MgH<sub>2</sub> overall dehydriding enthalpy is reduced from 76.5 kJ/mol H<sub>2</sub> to 69.1 kJ/mol H<sub>2</sub>. This last value allowed us to estimate the formation enthalpy of AgMg<sub>4</sub> at –59.5 kJ/mol.

Besides destabilization, a slight improvement in hydrogen absorption kinetics and a more noticeable enhancement in desorption kinetics has been observed in samples containing Ag as an additive. During thermal desorption, the dehydriding temperature decreases by 20 °C. In isothermal desorption experiments at 325 °C, the characteristic induction period of MgH<sub>2</sub> without additive practically disappears, and the time to reach 50% of conversion decreases from 17 min to 5.4 min when silver is present. The changes in desorption kinetics could be attributed to AgMg or the interfaces MgH<sub>2</sub>/AgMg acting as nucleation sites for Mg.

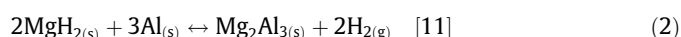
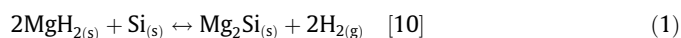
© 2014 Elsevier B.V. All rights reserved.

## 1. Introduction

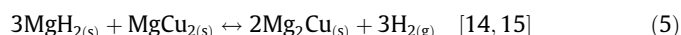
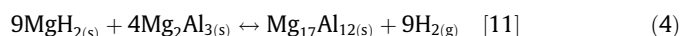
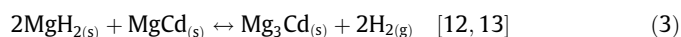
Mg-based materials have been extensively studied in the last years, due to their potential application to store hydrogen [1–6]. The high storage capacity by weight of magnesium, its low cost, and the reversibility of the reaction are the main advantages of these materials. On the other hand, the slow hydrogen absorption and desorption rates near room temperature, and the high stability of the hydride constitute their major drawbacks. Many efforts have been devoted to obtain Mg-based materials with better kinetics. The incorporation of additives that act as catalysts [3,5–7], and the modification of the microstructure by mechanical alloying [5,8,9] are successful examples of improvements. However, the problems associated with the high stability of magnesium hydride, such as the high equilibrium temperature at 1 bar of H<sub>2</sub>, still remain.

Thermodynamic destabilization has been the principal strategy explored to reduce the overall reaction enthalpy of desorption and hence, to decrease the equilibrium temperature of MgH<sub>2</sub> [4,10]. Thermodynamic destabilization employs an alternative route for

the decomposition and formation of the hydride. In particular, in the case of destabilization due to the formation of binary intermetallic compounds, two kinds of reactions can be distinguished: (a) processes in which MgH<sub>2</sub> reacts with a metal/semimetal during dehydrogenation forming a binary compound, and (b) routes in which MgH<sub>2</sub> reacts with an intermetallic compound producing another intermetallic after dehydrogenation. As examples of the first type of reactions we can mention [10,11]:



And as illustrations of the second type of destabilization [11–15]:



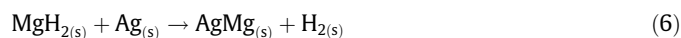
The second type of reactions could only take place in Mg–M systems where magnesium forms at least two binary compounds or alloys with M.

\* Corresponding author. Tel.: +54 294 4445100; fax: +54 2944 445199.

E-mail addresses: [urreta@cab.cnea.gov.ar](mailto:urreta@cab.cnea.gov.ar) (G. Urretavizcaya), [anasarmiento9@gmail.com](mailto:anasarmiento9@gmail.com) (A.C. Sarmiento Chávez), [fcastro@cab.cnea.gov.ar](mailto:fcastro@cab.cnea.gov.ar) (F.J. Castro).

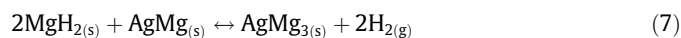
The Ag–Mg system is interesting for both types of destabilizing reactions, thanks to the existence of five intermetallic compounds formed by Ag and Mg [16,17]. The reported compounds are:  $\text{Ag}_3\text{Mg}$  (an ordered intermediate phase in the solid solution of Mg in Ag),  $\text{AgMg}$ , two phases with compositions near  $\text{AgMg}_3$  named  $\varepsilon$  ( $\text{Ag}_{7.96}\text{Mg}_{25.04}$ , low temperature phase) and  $\varepsilon'$  ( $\text{Ag}_{17}\text{Mg}_{54}$ , high temperature phase), and the intermetallic phase  $\text{Ag}_{9.01}\text{Mg}_{36.81}$ , for simplicity referred as  $\text{AgMg}_4$  hereinafter. As an additional attractive characteristic, Ag is the metal with the highest thermal conductivity. Hence, its incorporation to Mg could produce as an extra benefit an improvement in the thermal conductivity of the hydride bed, a well-known problem for the use of Mg as a  $\text{H}_2$  storage means [18].

The destabilization of  $\text{MgH}_2$  by metallic Ag could take place following the reaction:



The standard enthalpy of formation of  $\text{AgMg}$ , calculated from data in [16,19] gives  $-37.0$  kJ/mol.<sup>1</sup> Therefore, the decomposition of  $\text{MgH}_2$  through formation of  $\text{AgMg}$  could take place with an overall dehydriding enthalpy of  $39.1$  kJ/mol, a much lower value than  $76.1$  kJ/mol (standard  $\text{MgH}_2$  dehydriding enthalpy, direct reaction [20]). With this enthalpy value, we estimate for reaction (6) an equilibrium temperature of approximately  $-15$  °C at 1 bar of  $\text{H}_2$ , and an equilibrium pressure of 9.2 bar at room temperature. Therefore, this system can be considered as a promising candidate for hydrogen storage, although the Ag content significantly lowers its capacity and increases its cost. To the best of our knowledge, there are no literature reports analyzing  $\text{MgH}_2$  decomposition according to reaction (6). Only the reverse reaction has been explored [21], but not in the context of the destabilization of  $\text{MgH}_2$ . Unfortunately, Hwang et al. in [21] have reported that despite having tried to hydride  $\text{AgMg}$ , the compound have not absorbed hydrogen between 300 and 400 °C at hydrogen pressures up to 20 bar. Only if they added Ti or V, some hydrogen absorption was observed, but it has been attributed to the formation of Ti or V hydrides. However, according to the above estimation for the enthalpy change during reaction (6), the conditions used to hydride  $\text{AgMg}$  in [21] would be in the region of  $\text{AgMg}$  stability, and hence, hydriding of the alloy would not be expected. Therefore, it is very interesting to analyze if reaction (6) can be experimentally observed under convenient temperature and  $\text{H}_2$  pressure conditions.

$\text{MgH}_2$  could also be destabilized by a reaction involving two intermetallic compounds. Recently, Si et al. [22] have explored the hydriding and dehydriding processes of  $\text{AgMg}_3$  and have found that  $\text{MgH}_2$  can be slightly destabilized by the reaction:



In their paper they show that this reaction is reversible, and report  $\Delta H$  values of  $-68.2$  and  $69.8$  kJ/mol  $\text{H}_2$  for hydrogen absorption and desorption, respectively. Additionally, the material presents good cyclic stability.

Reaction (7) is just an example relating two of the five Ag–Mg intermetallic compounds. Many other reactions are in principle possible, involving different combinations of them. Nevertheless, the incomplete thermodynamic information about the Ag–Mg intermetallic compounds hinders the prediction of all the feasible reactions and the magnitude of the potential destabilizations.

In this paper we report the results of the investigation of both kinds of reactions: the reaction of  $\text{MgH}_2$  with Ag to give  $\text{AgMg}$ , and the reaction of  $\text{MgH}_2$  with  $\text{AgMg}$  to produce  $\text{AgMg}_4$ . In the first case only the forward reaction could be confirmed, whereas in the

second case it has been possible to reversibly follow the destabilized route. We therefore characterize these alternatives, and establish the thermodynamic and kinetic properties of the second reaction.

## 2. Experimental details

The materials were prepared by mechanically milling mixtures of pure raw materials.  $\text{MgH}_2$  (hydrogen storage grade) and Ag ( $2\text{--}3.5$   $\mu\text{m}$ , 99.9+ %) were purchased from Sigma–Aldrich, while Mg (99%) was purchased from Riedel de Haën. For the first part of the study, the analysis of reactions between  $\text{MgH}_2$  and Ag, two mixtures were prepared: an equimolar mixture of magnesium and silver, and an equimolar mixture of magnesium hydride and silver. Both mixtures were milled in a low-energy mill (Uniball Mill II, Australian Scientific Instruments) under pure argon atmosphere (99.999%) for 100 h. The milling settings were: 0.1 MPa of argon pressure, ball-to-powder mass ratio equal to 44:1, double magnet of the milling device in the bottom position, and rotational speed of 196 rpm. For the second part of the study, the analysis of reactions between  $\text{MgH}_2$  and  $\text{AgMg}$ , a mixture of magnesium hydride with 2.7 mol.% of Ag was milled in a planetary mill (Fritsch Monomill Pulverisette 6) under pure hydrogen atmosphere (99.999%) during 10 h. Magnesium hydride without additive was also milled in the same conditions for comparison. These samples will be referred hereinafter as  $\text{MgH}_2/\text{Ag}$  and  $\text{MgH}_2/\text{ref}$ , respectively. The milling conditions were: 0.5 MPa of hydrogen pressure, ball-to-powder mass ratio equal to 40:1, rotational speed of 300 rpm, and steps of 10 min of milling followed by 20 min of pause.

The samples were always handled inside a glovebox under controlled Ar atmosphere ( $\text{O}_2$  and  $\text{H}_2\text{O} < 1$  ppm). XRD analyses were performed in a PW 1710/01, Philips Electronic Instruments diffractometer, with monochromated Cu K $\alpha$  radiation. For XRD measurements, the samples were prepared in an environmental chamber filled with Ar, later attached to the diffractometer. The material crystallite size was estimated using the Scherrer equation [23], after subtracting the instrumental contribution. Surface area measurements were performed in a Micromeritics ASAP 2020 equipment. SEM observations were carried out in a SEM 515, Philips Electronic Instruments microscope. DSC runs were performed in a TA Instruments 2910 apparatus at a 6 °C/min heating rate under 122 ml/min argon flow. Treatments under hydrogen atmosphere, hydrogen sorption kinetics and equilibrium measurements were performed in a custom-made volumetric equipment. Hydriding kinetics data were measured at 325 °C and 300 °C with a  $\text{H}_2$  pressure of 1 MPa. Desorption curves were registered at 325 °C and 0.030 MPa of  $\text{H}_2$ . Before the first desorption, the as-milled samples were heated under 3 MPa  $\text{H}_2$  up to 325 °C. Desorption isotherms were measured at 300, 325 and 350 °C on hydrogen-cycled samples.

## 3. Results and discussion

### 3.1. Reaction of $\text{MgH}_2$ with Ag

As mentioned in the introduction, we have estimated that the reaction of Ag and  $\text{MgH}_2$  to give  $\text{AgMg}$  and  $\text{H}_2$  as products according to reaction (6) reduces the overall dehydriding enthalpy of  $\text{MgH}_2$  from  $76.1$  kJ/mol to  $39.1$  kJ/mol. In the corresponding van't Hoff diagram (Fig. 1) can be seen that, based on these calculations, this destabilized route significantly reduces the hydriding/dehydriding equilibrium temperature at 1 bar of  $\text{H}_2$ . To experimentally analyze the feasibility of this reaction, an equimolar mixture of  $\text{MgH}_2$  and Ag was milled under Ar atmosphere for 100 h. After milling, an appreciable amount of  $\text{AgMg}$  (ICDD PDF Card 65-220, Table 1) was registered (Fig. 2b) together with Ag (ICDD PDF Card 4-783, Table 1) and a bit of unreacted  $\beta\text{-MgH}_2$  (ICDD PDF Card 12-697). The Ag peaks are slightly shifted due to the solution of Mg in the lattice. From the lattice parameter value estimated at  $4.126$  Å and the changes in cell parameters of this phase as a function of Mg content given in [16], we estimate that 37 at.% Mg is dissolved into Ag. This value exceeds the equilibrium solid solubility limit, but as is extensively reported in [24], is usual to observe supersaturated solutions in non-equilibrium mechanically milled materials.

The clear observation of  $\text{AgMg}$  reflections shows that reaction (6) has taken place in a great extent during milling. The total conversion to  $\text{AgMg}$  can be achieved with a short heat treatment. A DSC run of the milled material (Fig. 3) presents an endothermic event that is attributed to the completion of reaction (6), as was

<sup>1</sup> The Ag destabilization of  $\text{MgH}_2$  by reactions that involve other Ag–Mg intermetallics cannot be analyzed due to the lack of thermodynamic information.

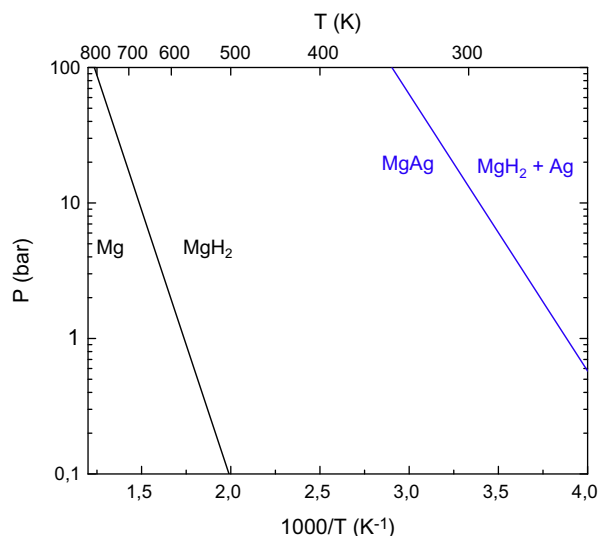


**Fig. 1.** Calculated van't Hoff plots of the reactions  $\text{Mg} + \text{H}_2 \leftrightarrow \text{MgH}_2$  and  $\text{AgMg} + \text{H}_2 \leftrightarrow \text{Ag} + \text{MgH}_2$  based on thermodynamic data published in [16,19,20].

**Table 1**

Structural parameters of Ag, AgMg and AgMg<sub>4</sub> from the ICDD PDF Cards 4-783, 65-3220 and 73-5691, respectively.

Phase	Space group	Lattice parameters		
		a (Å)	b (Å)	c (Å)
Ag	Fm-3m	4.086	4.086	4.086
AgMg	Pm-3m	3.311	3.311	3.311
AgMg <sub>4</sub>	P63/m	12.485	12.485	14.412

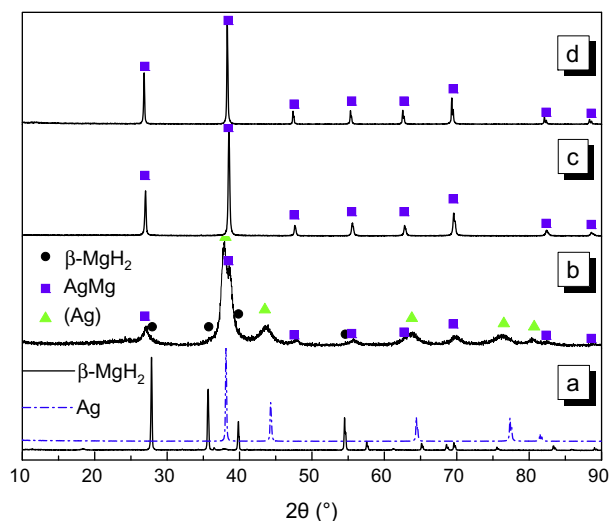


**Fig. 2.** Powder X-ray diffraction patterns of (a) starting  $\text{MgH}_2$  and Ag, (b) as-milled equimolar mixture of  $\text{MgH}_2$  and Ag, (c) the same material after DSC measurement and (d) the milled equimolar mixture after heat treatment under Ar.

confirmed by XRD (Fig. 2c). The percentage of the initial  $\text{MgH}_2$  that reacts during this event is determined using the area under the DSC curve and the enthalpy value of reaction (6) calculated above (39.1 kJ/mol). This amount is estimated at 9%, confirming that a large amount of the original  $\text{MgH}_2$  has reacted during milling (91%). The maximum heat flow was observed at 275 °C, 85 °C below the characteristic temperature of direct decomposition of  $\text{MgH}_2/\text{ref}$  (Fig. 3). The reduction in the decomposition temperature is a consequence of the destabilization of  $\text{MgH}_2$  by Ag.

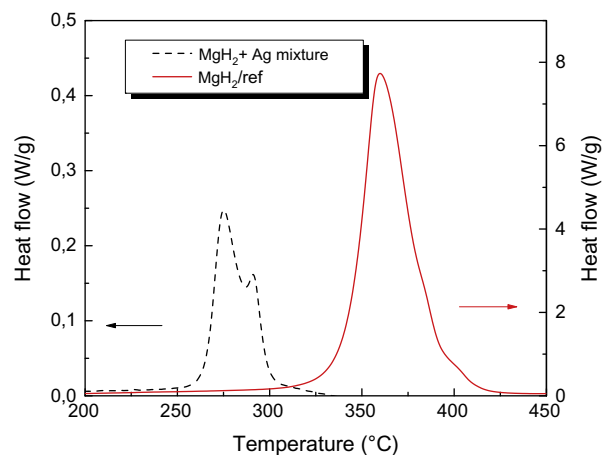


**Fig. 3.** DSC traces of the as-milled equimolar mixture of  $\text{MgH}_2$  and Ag (dashed line); and  $\text{MgH}_2/\text{ref}$  (solid line).

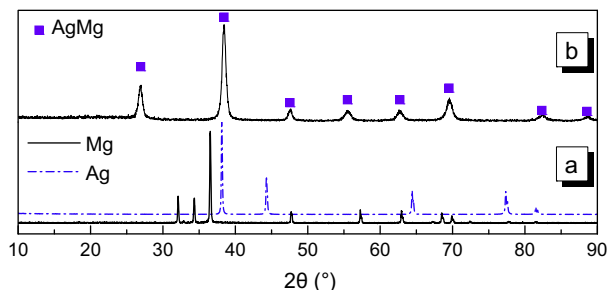


**Fig. 4.** Powder X-ray diffraction patterns of (a) starting Mg and Ag and (b) as-milled equimolar mixture of Mg and Ag.

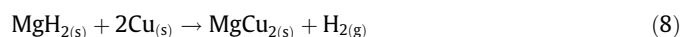
Nevertheless, this temperature is well above the thermodynamically predicted temperature, suggesting that the process occurs under a kinetic restriction.

To analyze if reaction (6) occurs in the reverse direction, the formation of AgMg was first completed keeping the milled material at 400 °C for 5 h, under Ar atmosphere. After this treatment, AgMg was the sole phase identified by XRD (Fig. 2d). The corresponding crystallite size was estimated at 40 nm. The hydriding of AgMg was attempted by two different cycling treatments in a volumetric device. During the first one, a sample was cycled in temperature between RT and 300 °C under 6 MPa of hydrogen (5 cycles). During the second one, a sample was cycled 10 times in pressure between vacuum and 6 MPa of  $\text{H}_2$  at 50 °C. After this, it was kept 17 h under 6 MPa of  $\text{H}_2$  at 50 °C. No hydrogen absorption was registered during these experiments. The absence of reaction was independently confirmed by the absence of thermal events in DSC runs and the lack of  $\text{MgH}_2$  peaks in XRD analyses done on the cycled samples.

The heat treatment used to complete the formation of AgMg has the additional effect of modifying the microstructural characteristics acquired during milling. It is known that these characteristics facilitate the hydriding process. Typically, the thermal treatments diminish defects concentration, increases crystallite size, etc. To avoid these effects, we have also tried to hydride as-milled AgMg. To this end, an equimolar mixture of Mg and Ag was milled under Ar atmosphere. After 100 h of milling, the only product was AgMg (Fig. 4b). The wider diffraction peaks indicate a more favorable microstructure. Scherrer's crystallite size gave a value of 14 nm. Despite this difference, it was impossible to hydride this material with the cycling treatments. We even tried hydriding AgMg directly by reactive mechanical alloying. We subjected the AgMg previously obtained by milling Ag and Mg to 10 h of additional

milling under 1 MPa of H<sub>2</sub> in a P6 apparatus. Also in this case the results were negative. It seems that AgMg cannot be hydrided in the explored conditions due to kinetic restrictions combined with experimental limitations. Pressures exceeding 10 MPa are required to hydride AgMg even at a moderate temperature of 70 °C. As our experimental device cannot exceed 6 MPa, we are limited to a maximum temperature of 60 °C to remain on the MgH<sub>2</sub> stability side of the van't Hoff diagram. Evidently, this temperature is not high enough for the reverse of reaction (6) to proceed at an appreciable rate. We conclude then that it is essential to improve the kinetics of this reaction in order to observe it experimentally.

It is interesting to compare these observations with the properties of other Mg–M systems, where M is a metal from the same group or period that Ag in the periodic table (Table 2). Strong similarities are found between the Mg–Ag system and the Mg–Cu system. Mg forms only two intermetallic compounds with Cu: Mg<sub>2</sub>Cu and MgCu<sub>2</sub>, and under equilibrium conditions the only destabilized reaction of MgH<sub>2</sub> with Cu is:



The standard dehydriding enthalpy of MgH<sub>2</sub> following this route is estimated to be 41 kJ/mol H<sub>2</sub>, a very similar value to that of reaction (6) in the Mg–Ag system. As a consequence of this, an equilibrium temperature at 1 bar H<sub>2</sub> of 39 °C is predicted for this reaction. In this condition the system is potentially applicable as a hydrogen storage media. Reaction (8) has been reported in a mechanically milled mixture of MgH<sub>2</sub> and Cu [25], in a process similar to the one reported here. It has also been mentioned to have taken place in Mg/Cu superlaminates [26]. To the best of our knowledge, there are no reports that reaction (8) occurs in the reverse direction. Only in [14] it is mentioned that MgCu<sub>2</sub> does not take up hydrogen at temperatures up to 350 °C and H<sub>2</sub> pressures of 2.3 MPa, but considering the van't Hoff diagram for this reaction, MgCu<sub>2</sub> is expected to react with H<sub>2</sub> at this pressure at temperatures below 127 °C.

When M is a Ag neighbor in the same period of the periodic table, the similarities between the Mg–Ag and Mg–M systems are less pronounced. Cd and In, for instance, destabilize MgH<sub>2</sub> decomposition in a lesser degree, presenting dehydriding enthalpies of the order of 60 kJ/mol H<sub>2</sub>. On the contrary, Pd destabilizes MgH<sub>2</sub> so strongly that is practically impossible to hydride the intermetallic compound MgPd. This is in agreement with the presence of MgPd in fully hydrided Mg/Pd materials [30]. The reversible absorption and desorption of H<sub>2</sub> by a destabilized route has only been confirmed experimentally for these systems in Mg–Cd (reaction involving Mg<sub>3</sub>Cd) [12,13], and partially in Mg–In [28,31].

### 3.2. Reaction of MgH<sub>2</sub> with AgMg

The other option to destabilize MgH<sub>2</sub> is to induce the reaction of the hydride with an Ag–Mg intermetallic and obtain another

intermetallic and gaseous H<sub>2</sub> as products. To explore this alternative we prepared a mixture of MgH<sub>2</sub> and AgMg by first milling MgH<sub>2</sub> and Ag (2.7 mol.%) and then performing a thermal treatment. After that, we analyzed the interaction of this material with H<sub>2</sub>.

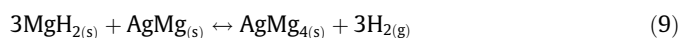
#### 3.2.1. Characterization of the as-milled materials

After milling, the XRD diagram of MgH<sub>2</sub>/Ag (Fig. 5b) shows the characteristic reflections of β-MgH<sub>2</sub> (ICDD PDF Card 12–697), metastable γ-MgH<sub>2</sub> (ICDD PDF Card 35–1184), metallic Ag (ICDD PDF Card 4–783), a small contribution from MgO (ICDD PDF Card 45–946), and a tiny shoulder corresponding to AgMg (insert). However, after a short heat treatment consisting of heating up the sample to 325 °C in 90 min under 3 MPa of H<sub>2</sub>, the AgMg peaks are clearly visible, and those of Ag disappear (Fig. 5d). Therefore, after this heat treatment, the sample is totally converted to a mixture of MgH<sub>2</sub> and AgMg. The XRD diagram of MgH<sub>2</sub>/ref (Fig. 5c) shows β-MgH<sub>2</sub>, and γ-MgH<sub>2</sub> reflections and a small signal from MgO. Peak shapes are similar to those of MgH<sub>2</sub>/Ag. Peak broadening is due in both cases to microstructural refinement induced by mechanical milling [5]. Scherrer's crystallite size in the two materials is around 10 nm. The observation of metastable γ-MgH<sub>2</sub> is a typical consequence of milling MgH<sub>2</sub> [32], and the presence of MgO can be attributed to the high reactivity of MgH<sub>2</sub> to O<sub>2</sub> that is present in ppm levels in the milling vessel and in the glovebox.

The morphological changes produced by milling are similar for MgH<sub>2</sub>/ref and MgH<sub>2</sub>/Ag. They mainly consist of an important decrease of the initial MgH<sub>2</sub> particle size. During milling, the elongated particles of 150–200 μm of the starting hydride (Fig. 6a) are repeatedly broken into smaller particles, presenting a final size in the range 1–20 μm (Fig. 6b and c). Both materials show a bimodal particle size distribution, with biggest particles ranging from 10 to 20 μm, and smallest ones with sizes around 1 μm. Microstructural and morphological similarities are accompanied by comparable BET specific surface areas, with values of 9 m<sup>2</sup>/g for both materials.

#### 3.2.2. Reaction with H<sub>2</sub>, equilibrium properties

The analysis of the interaction with hydrogen of the MgH<sub>2</sub>/Ag mixture was done on the heat treated material. The sample was first dehydrided at 325 °C under 0.03 MPa of H<sub>2</sub> and then rehydrided at the same temperature under 1 MPa H<sub>2</sub>. After the first desorption, an XRD pattern of the material (Fig. 7a) shows the presence of Mg (ICDD PDF Card 35–821) and AgMg<sub>4</sub> (ICDD PDF Card 73–5691, Table 1). The rehydrided material presents AgMg and β-MgH<sub>2</sub> (Fig. 7b). After subsequent desorptions and absorptions, the same products are identified, showing the reversibility of this dehydriding–hydriding route. The whole process can be described by:



This reaction occurs simultaneously with the direct reaction:



**Table 2**

Thermodynamic parameters of MgH<sub>2</sub> destabilized by different metals. ΔH and ΔS values have been calculated from thermodynamic information given in the indicated references.

System	Reaction	ΔH (kJ/mol H <sub>2</sub> )	ΔS (J/mol K)	T <sub>eq</sub> @ 1 bar H <sub>2</sub> (°C)	Refs.
Mg	MgH <sub>2(s)</sub> ↔ Mg <sub>(s)</sub> + H <sub>2(g)</sub>	76.1	132.3	302	[20]
Mg–Ag	MgH <sub>2(s)</sub> + Ag <sub>(s)</sub> ↔ AgMg <sub>(s)</sub> + H <sub>2(g)</sub>	39.1	151.8	–15	[16,19,20]
Mg–Cu	MgH <sub>2(s)</sub> + 2Cu <sub>(s)</sub> ↔ MgCu <sub>2(s)</sub> + H <sub>2(g)</sub>	41.0	131.3	39	[20]
Mg–Cd	3MgH <sub>2(s)</sub> + Cd <sub>(s)</sub> ↔ Mg <sub>3</sub> Cd <sub>(s)</sub> + 3H <sub>2(g)</sub>	68.6	130.9	251	[20,27]
	MgH <sub>2(s)</sub> + Cd <sub>(s)</sub> ↔ MgCd <sub>(s)</sub> + H <sub>2(g)</sub>	62.3	130.1	206	[20,27]
	MgH <sub>2(s)</sub> + 3Cd <sub>(s)</sub> ↔ MgCd <sub>3(s)</sub> + H <sub>2(g)</sub>	57.0	131.8	160	[20,27]
Mg–In	MgH <sub>2(s)</sub> + In <sub>(s)</sub> ↔ MgIn <sub>(s)</sub> + H <sub>2(g)</sub>	64.6	130.0 <sup>a</sup>	224	[20,28]
Mg–Pd	MgH <sub>2(s)</sub> + Pd <sub>(s)</sub> ↔ MgPd <sub>(s)</sub> + H <sub>2(g)</sub>	–74.5	130.0 <sup>a</sup>	–	[20,29]

<sup>a</sup> ΔS taken equal to 130 J/mol K due to the lack of S° values of MgIn and MgPd.



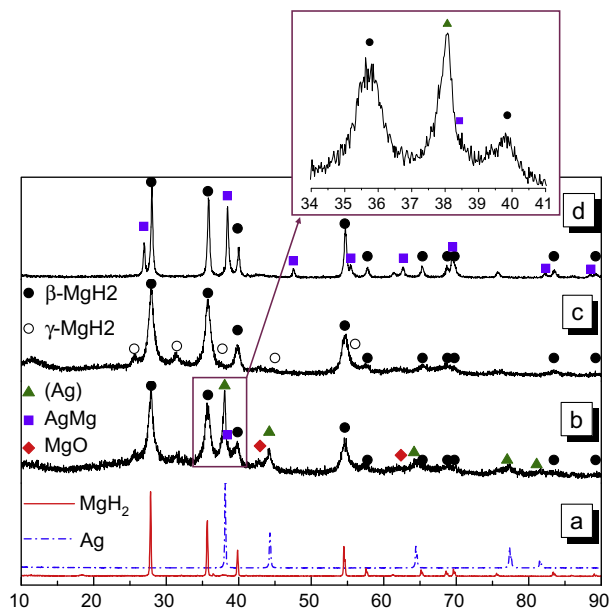
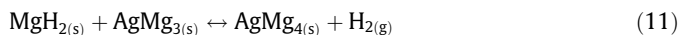


Fig. 5. Powder X-ray diffraction patterns of (a) starting materials  $\text{MgH}_2$  and Ag, (b)  $\text{MgH}_2/\text{Ag}$ , (c)  $\text{MgH}_2/\text{ref}$  and (d)  $\text{MgH}_2/\text{Ag}$  after heating up to  $325^\circ\text{C}$  under  $\text{H}_2$ .

To determine the enthalpy and entropy changes during reaction (9) desorption P–C isotherms were recorded in the temperature range  $300\text{--}350^\circ\text{C}$  (Fig. 8). All curves present two plateaux, showing that effectively the decomposition of  $\text{MgH}_2$  following the alternative route has different thermodynamic properties. The short plateau corresponds to hydrogen desorption according to reaction (9), whereas the long one relates to desorption following reaction (10). The length of each plateau is proportional to the amount of  $\text{MgH}_2$  and  $\text{AgMg}$  in the sample. The amount of  $\text{H}_2$  desorbed following reaction (9) is 8.5% of the total  $\text{H}_2$  desorbed, in excellent agreement with the calculated value of 8.6% considering the composition of the mixture. The van't Hoff plots obtained from both plateaux are shown in Fig. 9. The enthalpy and entropy of decomposition for  $\text{MgH}_2$  via reactions (9) and (10), determined by linear fitting are listed in Table 3.

The dehydriding enthalpy following reaction (9) is  $69.1\text{ kJ/mol H}_2$ , a value slightly minor than that of the direct reaction ( $76.5\text{ kJ/mol H}_2$ ), showing an effective, though small, destabilizing effect of  $\text{AgMg}$  in  $\text{MgH}_2$ . The magnitude of the change corresponds to a decrease of  $16^\circ\text{C}$  in the equilibrium desorption temperature at 1 bar of  $\text{H}_2$ . The extent of destabilization is similar to that found by Si et al. in the  $\text{AgMg}_3\text{--H}_2$  system [22]. In this work they have reported a value of  $69.8\text{ kJ/mol H}_2$  for the enthalpy of reaction (7). Taking this value into account, reaction (9) should be interpreted as a representation of the whole process, as the real reaction pathway might also involve reaction (7), which presents a similar equilibrium pressure due to the comparable  $\Delta H$  values. If reaction (7) actually took place during the high pressure plateau, as the only phase identified after dehydriding was  $\text{AgMg}_4$ , the following reaction should also have occurred:



From the desorption enthalpies of reactions (7) and (9), we estimate the corresponding value for reaction (11) at  $67.7\text{ kJ/mol H}_2$ , predicting an equilibrium pressure also in the range of the high pressure plateau.

The degree of  $\text{MgH}_2$  destabilization induced by  $\text{AgMg}$  and  $\text{AgMg}_4$  is also similar to the one produced by different Mg–M

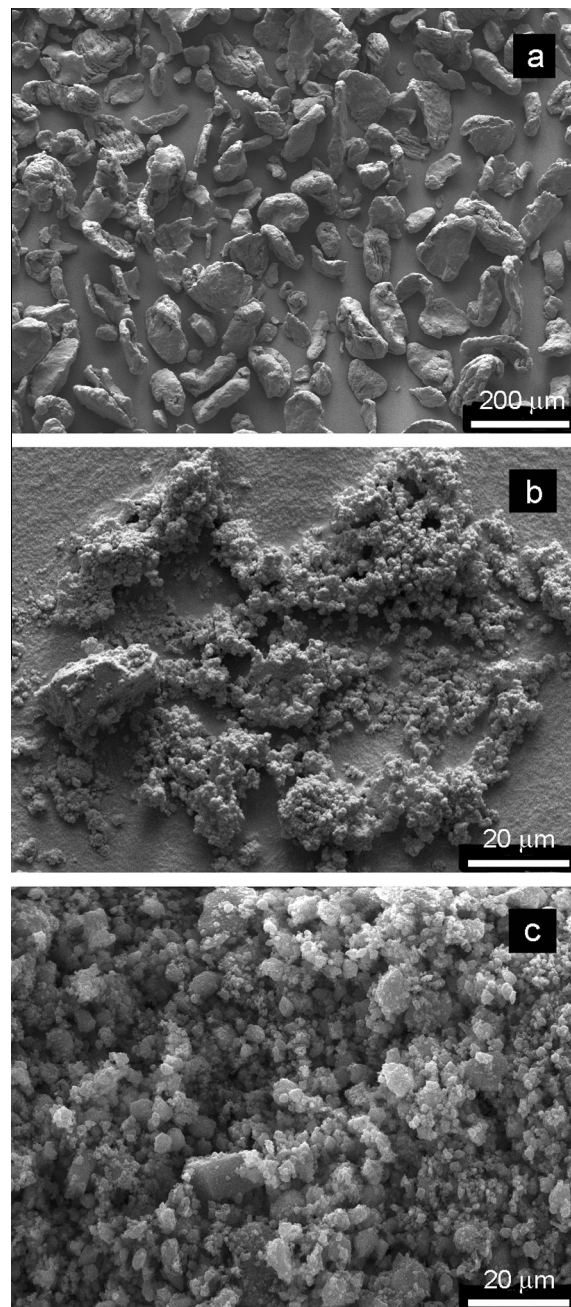
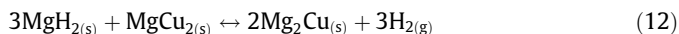


Fig. 6. SEM images of (a) starting  $\text{MgH}_2$ , (b)  $\text{MgH}_2/\text{ref}$  and (c)  $\text{MgH}_2/\text{Ag}$ .

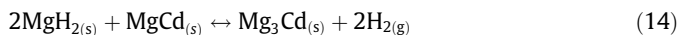
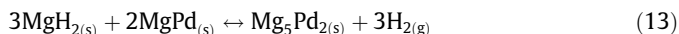
intermetallics, with M a close neighbor of Ag in the periodic table (Table 4).

In the Mg–Cu system,  $\text{MgH}_2$  can be destabilized by  $\text{MgCu}_2$  and  $\text{Mg}_2\text{Cu}$  according to reaction (12) [14,15]:



The enthalpy changes measured in this case are also small, and the reduction in the equilibrium temperature is of the same order of magnitude that the one reported here.

In the Mg–Pd and Mg–Cd systems reactions analogous to (9) have been observed [12,13,30]:



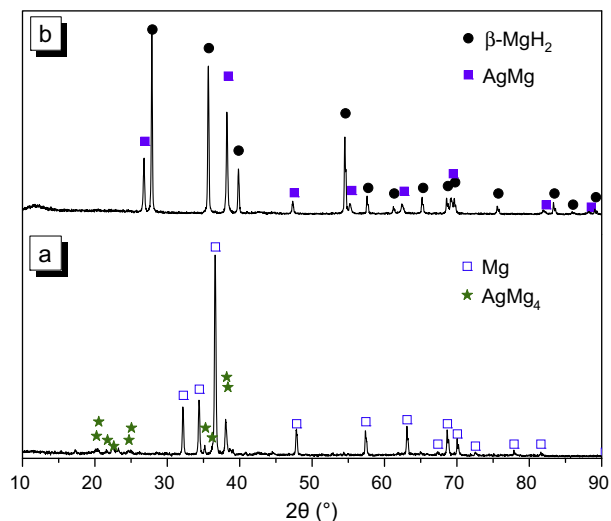


Fig. 7. Powder X-ray diffraction patterns of MgH<sub>2</sub>/Ag after H<sub>2</sub> cycling: (a) dehydrided and (b) hydrided.

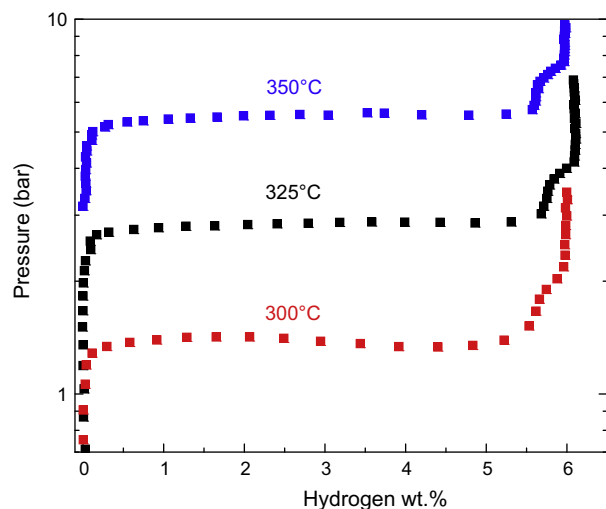
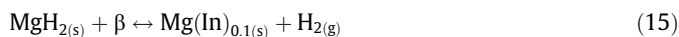


Fig. 8. Pressure – composition desorption isotherms of MgH<sub>2</sub>/Ag measured at different temperatures.

The enthalpy change for reaction (13) is 90.17 kJ/mol H<sub>2</sub>. This value is higher than that of MgH<sub>2</sub>/Mg. However, Huot et al. have reported that reaction (13) destabilizes MgH<sub>2</sub> at 200 °C [30]. The apparent discrepancy could be attributed to the entropy change of the reaction. Unfortunately, this value has not been measured and cannot be calculated with the available data. On the other hand, the enthalpy changes with MgCd destabilized MgH<sub>2</sub> (reaction 14) are between 5 and 10 kJ/mol H<sub>2</sub> below the direct reaction value [20], as it happens with AgMg.

In the Mg–In system the destabilized reported reactions can be represented by:



where  $\beta$  denotes several possible Mg–In intermetallic phases including Mg<sub>3</sub>In, Mg<sub>2</sub>In and MgIn [28,31]. In these cases also, the magnitude of the destabilization is similar to the one observed with AgMg (Table 4).

The MgH<sub>2</sub> dehydriding enthalpy value determined here following reaction (9) allows us to estimate the AgMg<sub>4</sub> formation enthalpy. To the best of our knowledge, this value is not reported

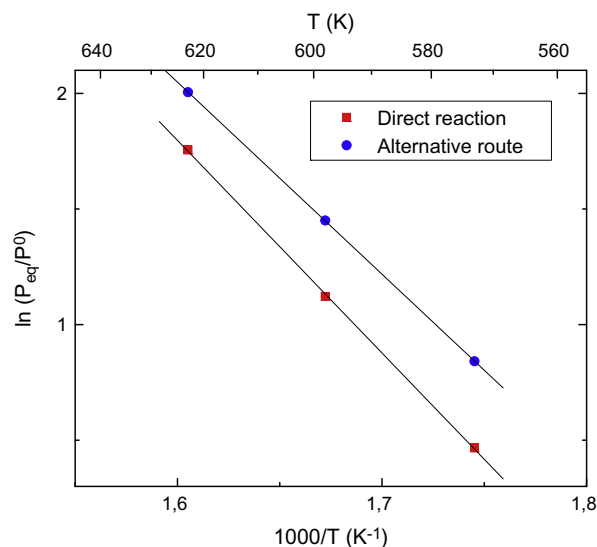


Fig. 9. van't Hoff plots of the reactions  $\text{AgMg}_4 + 3 \text{H}_2 \leftrightarrow 3 \text{MgH}_2 + \text{AgMg}$  and  $\text{Mg} + \text{H}_2 \leftrightarrow \text{MgH}_2$ .

Table 3

Enthalpy and entropy changes obtained from van't Hoff plots of Fig. 9.

Reaction	$\Delta H$ (kJ/mol H <sub>2</sub> )	$\Delta S$ (J/mol K)
Direct (10)	76.5	137.3
$\text{MgH}_{2(s)} \leftrightarrow \text{Mg}_{(s)} + \text{H}_{2(g)}$		
Alternative route (9)	69.1	127.5
$3\text{MgH}_{2(s)} + \text{AgMg}_{(s)} \leftrightarrow \text{AgMg}_{4(s)} + 3\text{H}_{2(g)}$		

in the literature. Using the enthalpy value determined here for reaction (9) and the AgMg formation enthalpy at 298 K calculated from data in [16,19] we obtained a AgMg<sub>4</sub> formation enthalpy equal to −59.5 kJ/mol.

### 3.2.3. Reaction with H<sub>2</sub>, kinetic properties

Reaction kinetics has been studied by isothermal hydrogen absorption and desorption experiments in a volumetric device, and by DSC. The isothermal desorption curves (Fig. 10a) show that dehydriding in MgH<sub>2</sub>/Ag happens at a rate three times faster than in MgH<sub>2</sub>/ref. The required time to desorb 3 wt.% of hydrogen decreases from 16 min for MgH<sub>2</sub>/ref to 5.5 min for MgH<sub>2</sub>/Ag. In addition to the shortening of the reaction time, another advantageous difference in the MgH<sub>2</sub>/Ag desorption curves is the substantial reduction of the induction period. It seems that AgMg, or the MgH<sub>2</sub>/AgMg interfaces could be improving the Mg nucleation rate by providing special nucleation sites and hence facilitating the starting of desorption. A similar trend has been observed by DSC. The curves (Fig. 11) show that the presence of Ag improves desorption, shifting the DSC peak approximately 20 °C to lower temperatures in comparison to the MgH<sub>2</sub>/ref peak.

Isothermal absorption kinetics is slightly better in the sample with additive (Fig. 10b). Roughly 1.7 min are required to absorb 4 wt.% of hydrogen at 325 °C in MgH<sub>2</sub>/Ag, whereas 2 min are required in MgH<sub>2</sub>/ref. Interestingly, a small improvement in hydrogen absorption at 300 °C has been found in this work, in contrast to previous results reported in [33]. We achieved a conversion degree equal to 0.97 after 10 min under a H<sub>2</sub> pressure of 1 MPa (Fig. 7b), whereas a conversion of only 0.25 after 10 min at 3 MPa H<sub>2</sub> has been reported in [33] for a similar material (Mg/2 mol.% Ag, milled under Ar). Perhaps, in this last case, the limited hydriding could be attributed to a passivity procedure made on the samples before measurements.

**Table 4**

Measured thermodynamic parameters of  $\text{MgH}_2$  destabilized by different intermetallic compounds. Equilibrium temperatures at 1 bar  $\text{H}_2$  ( $T_{\text{eq}}$ ) were calculated using reported  $\Delta H$  and  $\Delta S$  values. In the case of Mg–Pd system, the  $\Delta H$  value was calculated using data from [20,29].

System	Reaction	$\Delta H$ (kJ/mol $\text{H}_2$ )	$\Delta S$ (J/mol K)	$T_{\text{eq}}$ @ 1 bar $\text{H}_2$ ( $^{\circ}\text{C}$ )	Refs.
Mg	$\text{MgH}_{2(s)} \leftrightarrow \text{Mg}_{(s)} + \text{H}_{2(g)}$	76.1	132.3	302	[21]
Mg–Ag	$3\text{MgH}_{2(s)} + \text{AgMg}_{(s)} \leftrightarrow \text{AgMg}_{4(s)} + 3\text{H}_{2(g)}$	69.1	127.5	268	This work
	$2\text{MgH}_{2(s)} + \text{AgMg}_{(s)} \leftrightarrow \text{AgMg}_{3(s)} + 2\text{H}_{2(g)}$	69.8	Not reported	–	[22]
Mg–Cu	$3\text{MgH}_{2(s)} + \text{MgCu}_{2(s)} \leftrightarrow 2\text{Mg}_2\text{Cu}_{(s)} + 3\text{H}_{2(g)}$	72.8	142.3	293	[14]
		77.11	146.4	254	[15]
Mg–Pd	$3\text{MgH}_{2(s)} + 2\text{MgPd}_{(s)} \leftrightarrow \text{Mg}_5\text{Pd}_{2(s)} + 3\text{H}_{2(g)}$	90.17	–	–	Calculated from [20,29]
Mg–Cd	$2\text{MgH}_{2(s)} + \text{MgCd}_{(s)} \leftrightarrow \text{Mg}_3\text{Cd}_{(s)} + 2\text{H}_{2(g)}$	65.2	Not reported	–	[12]
		71	Not reported	–	[13]
Mg–In	$\text{MgH}_{2(s)} + \beta \leftrightarrow \text{Mg}(\text{In})_{0.1(s)} + \text{H}_{2(g)}$ ( $\beta = \text{Mg}_3\text{In}$ , $\text{Mg}_2\text{In}$ and $\text{MgIn}$ )	68.1	Not reported	–	[17]
		70.87	Not reported	263	[18]

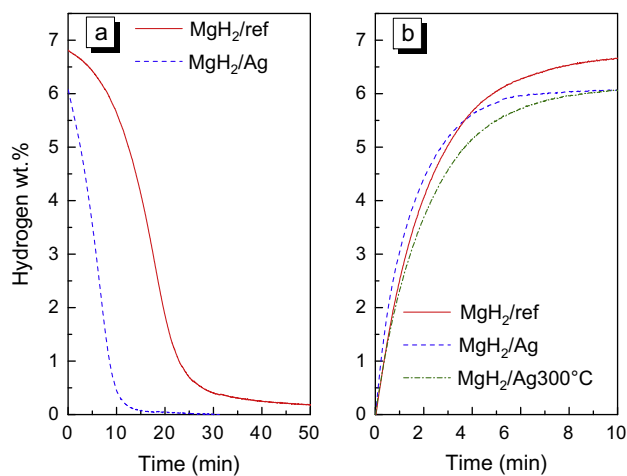


**Fig. 10.** (a) Isothermal hydrogen desorption (0.030 MPa  $\text{H}_2$ ) and (b) absorption (1 MPa  $\text{H}_2$ ) at 325  $^{\circ}\text{C}$ . The absorption curve at 300  $^{\circ}\text{C}$  in  $\text{MgH}_2/\text{Ag}$  is added for comparison (see text).

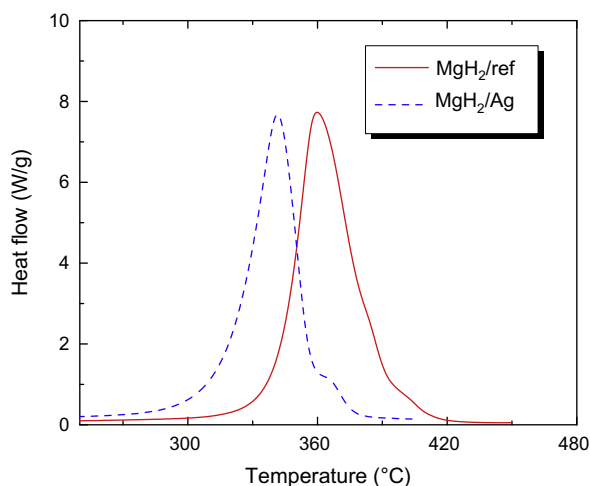


**Fig. 11.** DSC thermograms of  $\text{MgH}_2/\text{Ag}$  and  $\text{MgH}_2/\text{ref}$ .

#### 4. Conclusions

The absorption and desorption of  $\text{H}_2$  in the Mg–Ag system have been studied. We have found that  $\text{MgH}_2$  is destabilized either by Ag, producing  $\text{AgMg}$  and  $\text{H}_2$  as products, or by  $\text{AgMg}$ , giving  $\text{AgMg}_4$  and  $\text{H}_2$ .

In the first case the reaction has been observed only in the forward direction, i.e. it was not possible to rehydride  $\text{AgMg}$  in the explored conditions. We attribute this to an insufficient hydriding

rate at the temperature of the measurements (60  $^{\circ}\text{C}$ ). It was impossible to analyze  $\text{H}_2$  absorption at higher temperatures due to the combination of thermodynamic properties of the reaction and technical limitations in the experimental setup. Nevertheless, although with higher cost and lower capacity than magnesium, this system could be interesting for hydrogen storage if the kinetics could be improved.

In the second case the reaction occurs reversibly and with slightly better thermodynamic characteristics than the direct decomposition. The dehydriding enthalpy estimated from isothermal pressure–composition curves and a van't Hoff plot is 69.1 kJ/mol  $\text{H}_2$ , only 7.4 kJ/mol  $\text{H}_2$  below the respective value for the direct reaction. Using this value we could estimate the formation enthalpy of  $\text{AgMg}_4$  at  $-59.5$  kJ/mol. Besides destabilization, the addition of Ag produces a moderate improvement in the hydrogen desorption and absorption rates. The temperature of thermal desorption decreases 20  $^{\circ}\text{C}$  after Ag addition, and in isothermal volumetric measurements, the required time to achieve 50% of conversion during desorption at 325  $^{\circ}\text{C}$  decreases from 17 min to 5.4 min. Hydrogen absorption is practically the same in the materials with or without Ag. The kinetic improvement on desorption could be explained by the compound  $\text{AgMg}$  or the  $\text{MgH}_2/\text{AgMg}$  interfaces acting as nucleation sites for Mg. This phenomenon would be responsible of the significant reduction of the induction period observed in the desorption curves of the material milled with Ag.

Overall, the Mg–Ag system has shown a  $\text{H}_2$  absorption and desorption behavior similar to that of other Mg–M systems, with M a close neighbor of Ag in the periodic table of the elements.

#### Acknowledgments

Partial financial support from PAE-PICT No. 133 (ANPCyT), PIP 112 201101 00524 (CONICET) and Project 06/C399 (Universidad Nacional de Cuyo) is gratefully acknowledged.

#### References

- [1] L. Schlapbach, A. Züttel, Hydrogen storage materials for mobile applications, *Nature* 414 (2001) 353–358.
- [2] A. Züttel, Materials for hydrogen storage, *Mater. Today* 6 (2003) 24–33.
- [3] B. Sakintuna, F. Lamari-Darkrim, M. Hirscher, Metal hydride materials for solid hydrogen storage: a review, *Int. J. Hydrogen Energy* 32 (2007) 1121–1140.
- [4] M. Dornheim, S. Doppiu, G. Barkhordarian, U. Boesenberg, T. Klassen, O. Gutfleisch, Hydrogen storage in magnesium-based hydrides and hydride composites, *Scr. Mater.* 56 (2007) 841–846.
- [5] R.A. Varin, T. Czujko, Z.S. Wronski, *Nanomaterials for solid state hydrogen storage*, first ed., Springer, New York, 2009.
- [6] I.P. Jain, Ch. Lal, A. Jain, Hydrogen storage in Mg: a most promising material, *Int. J. Hydrogen Energy* 35 (2010) 5133–5144.
- [7] F. Tonus, V. Fuster, G. Urretavizcaya, F.J. Castro, J.L. Bobet, Catalytic effect of monoclinic  $\text{WO}_3$ , hexagonal  $\text{WO}_3$  and  $\text{H}_{0.23}\text{WO}_3$  on the hydrogen sorption properties of Mg, *Int. J. Hydrogen Energy* 34 (2009) 3404–3409.
- [8] J. Huot, G. Liang, S. Boily, A. van Neste, R. Schulz, Mechanical alloying of Mg–Ni compounds under hydrogen and inert atmosphere, *J. Alloys Comp.* 293–295 (1999) 495–500.

- [9] V. Fuster, F.J. Castro, H. Troiani, G. Urretavizcaya, Characterization of graphite catalytic effect in reactively ball-milled  $\text{MgH}_2$ -C and Mg-C composites, *Int. J. Hydrogen Energy* 36 (2011) 9051–9061.
- [10] J.J. Vajo, G.L. Olson, Hydrogen storage in destabilized chemical systems, *Scr. Mater.* 56 (2007) 829–834.
- [11] A. Andreassen, Hydrogenation properties of Mg–Al alloys, *Int. J. Hydrogen Energy* 33 (2008) 7489–7497.
- [12] V.M. Skripnyuk, E. Rabkin,  $\text{Mg}_3\text{Cd}$ : a model alloy for studying the destabilization of magnesium hydride, *Int. J. Hydrogen Energy* 37 (2012) 10724–10732.
- [13] G. Liang, R. Schulz, The reaction of hydrogen with Mg–Cd alloys prepared by mechanical alloying, *J. Mater. Sci.* 39 (2004) 1557–1562.
- [14] J.J. Reilly, R.H. Wiswall, The reaction of hydrogen with alloys of magnesium and copper, *Inorg. Chem.* 6 (1967) 2220–2222.
- [15] H. Shao, Y. Wang, H. Xu, X. Li, Preparation and hydrogen storage properties of nanostructured  $\text{Mg}_2\text{Cu}$  alloy, *J. Solid State Chem.* 178 (2005) 2211–2217.
- [16] A.A. Nayeib-Hashemi, J.B. Clark, The Ag–Mg (silver–magnesium) system, in: T.B. Massalski (Ed.), *Bulletin of Alloy Phase Diagrams*, second ed., Materials Park, ASM International, Ohio, 1984, pp. 348–358.
- [17] C. Kudla, Structurally complex intermetallic phases, Doctoral Thesis, Saxon State Library – Dresden State and University Library, Dresden, 2007.
- [18] A. Chaise, P. de Rango, Ph. Marty, D. Fruchart, S. Miraglia, R. Olivès, S. Garrier, Enhancement of hydrogen sorption in magnesium hydride using expanded natural graphite, *Int. J. Hydrogen Energy* 34 (2009) 8589–8596.
- [19] P.M. Robinson, M.B. Bever, The heat of formation of the intermetallic compound AgMg as a function of composition, *Trans. Met. Soc. AIME* 230 (1964) 1487–1488.
- [20] O. Kubaschewski, C.B. Alcock, P.J. Spencer, *Materials Thermochemistry*, sixth ed., Pergamon Press, Oxford, 1993.
- [21] S. Hwang, C. Nishimura, Synthesis of B2-structured Mg alloys by mechanical alloying, and their hydriding properties, *Mater. Sci. Forum* 386–388 (2002) 615–620.
- [22] T.Z. Si, J.B. Zhang, D.M. Liu, Q.A. Zhang, A new reversible  $\text{Mg}_3\text{Ag-H}_2$  system for hydrogen storage, *J. Alloys. Comp.* 581 (2013) 246–249.
- [23] H.P. Klug, L. Alexander, *X-ray Diffraction Procedures for Polycrystalline and Amorphous Materials*, second ed., John Wiley & Sons, New York, 1974.
- [24] C. Suryanarayana, Mechanical alloying and milling, *Prog. Mat. Sci.* 46 (2001) 1–184.
- [25] C.X. Shang, M. Bououdina, Y. Song, Z.X. Guo, Mechanical alloying and electronic simulations of  $(\text{MgH}_2 + \text{M})$  systems ( $\text{M} = \text{Al}, \text{Ti}, \text{Fe}, \text{Ni}, \text{Cu}$  and  $\text{Nb}$ ) for hydrogen storage, *Int. J. Hydrogen Energy* 29 (2004) 73–80.
- [26] K. Tanaka, H.T. Takeshita, K. Kurumatani, H. Miyamura, S. Kikuchi, The effect of initial structures of Mg/Cu super-laminates on hydrogen absorption/desorption properties, *J. Alloys. Comp.* 580 (2013) 5222–5225.
- [27] R. Hultgren, R.L. Orr, P.D. Anderson, K.K. Kelley, *Selected Values of Thermodynamic Properties of Metals and Alloys*, first ed., John Wiley & Sons, New York, 1963.
- [28] H.C. Zhong, H. Wang, J.W. Liu, D.L. Sun, M. Zhu, Altered desorption enthalpy of  $\text{MgH}_2$  by the reversible formation of Mg(In) solid solution, *Scr. Mater.* 65 (2011) 285–287.
- [29] J.F. Fernández, M. Widom, F. Cuevas, J. R. Ares, J. Bodega J, R. Leardini, M. Mihalkovic, C. Sánchez, First-principles phase stability calculations and estimation of finite temperature effects on pseudo-binary  $\text{Mg}_6(\text{Pd}_x\text{Ni}_{1-x})$  compounds, *Intermetallics* 19 (2010) 502–510.
- [30] J. Huot, A. Yonkeu, J. Dufour, Rietveld analysis of neutron powder diffraction of  $\text{Mg}_6\text{Pd}$  alloy at various hydriding stages, *J. Alloys Comp.* 475 (2009) 168–172.
- [31] Ch. Zhou, Z.Z. Fang, J. Lu, X. Zhang, Thermodynamic and kinetic destabilization of magnesium hydride using Mg–In solid solution alloys, *J. Am. Chem. Soc.* 135 (2013) 10982–10985.
- [32] F.C. Gennari, F.J. Castro, G. Urretavizcaya, Hydrogen desorption behavior from magnesium hydrides synthesized by reactive mechanical alloying, *J. Alloys Comp.* 321 (2001) 46–53.
- [33] A.F. Palacios-Lazcano, J.L. Luna-Sánchez, J. Jiménez-Gallegos, F. Cruz-Gandarilla, J.G. Cabañas-Moreno, Hydrogen storage in nanostructured Mg-base alloys, *J. Nano Res.* 5 (2009) 213–221.